



# Comparative study of new bone formation capability of zirconia bone graft material in rabbit calvarial

Ik-Jung Kim, Soo-Yeon Shin\*

Department of Prosthodontics, College of Dentistry, Dankook University, Cheonan, Republic of Korea

**PURPOSE.** The purpose of this study was to compare the new bone formation capability of zirconia with those of other synthetic bone grafts. **MATERIALS AND METHODS.** Twelve rabbits were used and four 6-mm diameter transcortical defects were formed on each calvaria. Each defect was filled with Osteon II (Os), Tigran PTG (Ti), and zirconia (Zi) bone grafts. For the control group, the defects were left unfilled. The rabbits were sacrificed at 2, 4, and 8 weeks. Specimens were analyzed through micro computed tomography (CT) and histomorphometric analysis. **RESULTS.** The Ti and Zi groups showed significant differences in the amount of newly formed bone between 2 and 4 weeks and between 2 and 8 weeks ( $P<.05$ ). The measurements of total bone using micro CT showed significant differences between the Os and Ti groups and between the Os and Zi groups at 2 and 8 weeks ( $P<.05$ ). Comparing by week in each group, the Ti group showed a significant difference between 4 and 8 weeks. Histomorphometric analysis also showed significant differences in new bone formation between the control group and the experimental groups at 2, 4, and 8 weeks ( $P<.05$ ). In the comparison of newly formed bone, significant differences were observed between 2 and 4 weeks and between 2 and 8 weeks ( $P<.05$ ) in all groups. **CONCLUSION.** Zirconia bone graft material showed satisfactory results in new bone formation and zirconia could be used as a new synthetic bone graft material. [*J Adv Prosthodont 2018;10:167-76*]

**KEYWORDS:** Zirconia; Titanium; Bone graft material; Newly formed bone

## INTRODUCTION

Many kinds of bone graft materials are being used for the reconstruction of defects in the oral and maxillofacial regions or for bone graft treatment accompanied by dental implant. Among these materials, autogenous bone has been considered a gold standard graft material with successful results.<sup>1</sup> However, autogenous bone has limitations, including morbidity of the donor site, insufficient amount of bone, and absorption during the healing period.<sup>2</sup> Although

allogenic and xenogenic bones have been used as substitutes for autogenous bone, these have the disadvantages of a possible immune response and the transmission of infectious disease.<sup>3,4</sup>

Recently, there has been remarkable progress in manufacturing techniques of bone substitute materials, and synthetic bone has been widely used; it has biological compatibility and osteoconduction that provides an excellent scaffold for the formation of new bones.<sup>5</sup> With the development of synthetic bone graft production technology, synthetic bone has become the main material for replacement of autogenous bone in dental operations.

Hydrate calcium phosphate synthetic bone, often referred to as hydroxyapatite, has biological compatibility and a structure that is similar to actual human cancellous bone.<sup>6</sup> However, hydroxyapatite is a biodegradable graft material in the human body and cannot maintain its original volume of graft.<sup>7</sup> Absorption of the grafted material leads to an unaesthetic result, especially in the anterior regions of mouth.

Titanium is commonly used as a dental implant as it has biocompatibility and is non-absorbable, and thus titanium bone graft material can maintain the volume of graft and

Corresponding author:  
Soo-Yeon Shin  
Department of Prosthodontics, College of Dentistry, Dankook University  
31116 Dandaero 119, Dongnam-gu, Cheonan 31116, Republic of Korea  
Tel. +8241 5500256; e-mail, syshin@dankook.ac.kr  
Received November 9, 2016 / Last Revision January 4, 2018 / Accepted  
February 27, 2018

© 2018 The Korean Academy of Prosthodontics  
This is an Open Access article distributed under the terms of the Creative Commons Attribution Non-Commercial License (<http://creativecommons.org/licenses/by-nc/3.0>) which permits unrestricted non-commercial use, distribution, and reproduction in any medium, provided the original work is properly cited.

alveolar bone.<sup>8,9</sup> However, titanium graft material cannot be used in the esthetic zone due to its unique metallic shade.<sup>10</sup>

Among the materials that can be used as bone grafts, zirconia is being studied as a material to replace existing alloplastic bone grafts and has shown excellent biological compatibility. Yttria-stabilized tetragonal zirconia polycrystals (Y-TZP) has excellent mechanical strength and biological compatibility.<sup>11-20</sup> Y-TZP is a non-absorbable material,<sup>21</sup> and with its color similar to those of natural teeth and alveolar bone, it can be used as bone substitute material in the anterior region of mouth and thin gingiva where esthetics are required.<sup>22</sup>

The production of a block bone graft that accurately fits an extensive defect is possible by capturing precise three-dimensional (3D) images of the bone defects using diagnostic imaging systems, such as 3D computed tomography (CT) and measuring the length, volume, and shape of the defect. The 3D imaging technology that is already being used for dental implants has excellent accuracy.<sup>23,24</sup> In comparison to other graft materials, zirconia is expected to play a better role as a block graft material because it is easier to manufacture and has a porous structure with an appropriate strength, and errors can be adjusted during the operation.

The ideal size and structure of synthetic bone graft materials have been reported in numerous studies. In most studies, a cribriform structure, which is similar to human bone, is recommended, and bone grafts with a granular shape have been designed for easy manipulation and control during bone graft surgery. Each granule has interconnected pores that maintain blood circulation and allow interaction among cells, thereby facilitating bone regeneration and bone growth. Although results are controversial, new bone formation is usually active at a pore size of 150 to 500  $\mu\text{m}$ ,<sup>25,26</sup> with the appropriate particle size of graft material for new bone formation being from 0.5 to 1.0 mm.<sup>27</sup>

The purpose of this study was to compare the new bone formation capability of zirconia with those of synthetic bone grafts. In this study, the 6 mm calvarial defects of New Zealand white rabbits were filled with synthetic, titanium, zirconia bone graft materials. After 2, 4 and 8 weeks, the newly formed bones of the groups were compared through micro CT and histomorphometric analysis.

## MATERIALS AND METHODS

A cribriform-shaped polyurethane was used to manufacture a zirconia porous scaffold (Filtrocell, Eurofoam, Troisdorf, Germany). The polyurethane was dipped in 2% NaOH solution for 30 minutes before being washed with distilled water. It was then stored for 24 hours at room temperature.

Zirconia powder 100 g (TZ-3Y-E, Tosoh Co., Yamaguchi, Japan) calcined at 600°C for 2 hours to remove impurities. Triethyl phosphate 6 g (TEP) was added to ethanol, which was then placed in a ball mill for 24 hours to produce a slurry. In this slurry, Polyvinyl butyral 6 g (PVB) was added, mixed, and then stored for 24 hours. The polyurethane that had been previously processed was dipped into the slurry

three times. To maintain the interconnected pore structure, the remaining slurry was removed by centrifuging at low speed and dried at 60°C for 10 minutes. This process was repeated twice, after which the polyurethane was kept at room temperature for 24 hours.

For sintering of this material, the temperature was increased to 600°C at the rate of 1°C per minute and then maintained for 2 hours to remove the polyurethane. The temperature was then increased again to 1550°C at the rate of 3°C per minute. After cooling, the zirconia graft material was placed in ethanol for 10 minutes and washed with an ultrasonic cleaner before being dried. The dried zirconia was crushed and made into granules, which were sorted by size using 0.5 and 1.0 mm with sieves. The granules were sterilized with ethylene oxide gas and stored in microtubes.

The titanium bone graft material (Tigran PTG, Tigran Technologies AB, Malmö, Sweden) consisted of porous titanium granules made of commercially pure titanium. The Ti granules were between 0.7 mm and 1.0 mm in size, irregularly shaped and non-resorbable. The granules have interconnected pores that provide a framework for new bone growth.

The synthetic bone graft material (Osteon II, Genoss Co., Suwon, Korea) was composed of hydroxyapatite 30% and beta-tricalcium phosphate 70%. It has an interconnected pore structure similar to that of human cancellous bone. The granules were between 0.5 mm and 1.0 mm in size.

This experiment received approval from the Institutional Animal Care and Use Committee (IACUC) of Cronex (CN20140528-1) and was conducted in accordance with the guidelines of the IACUC.

Twelve healthy New Zealand white male rabbits (weight 2.5 - 3.0 kg) were randomized into three groups. Each rabbit was anesthetized with 15 mg/kg of zoletil (VIRBAC S.A., Carros, France) and 5 mg/kg of xylazine (Bayer Korea Co., Ansan, Korea), and then 5 mg/kg of biotril (Komipharm Co., Shihung, Korea) was injected as a preoperative antibiotic. The hair of the rabbits was removed using an electric shaver, and the operation site was sterilized with a betadine solution before covering with a surgical drape. A midsagittal incision was made from the frontal region to the occipital region in the ventral position. The flap to the periosteum was retracted to the side. Four bone defects with a diameter of 6 mm were formed by using a trephine bur (Hager & Meisinger GmbH, Hanseemannstrasse, Germany) with careful drilling. One defect was unfilled for the control group, and three defects were grafted with Os, Ti, and Zi as bone graft materials. The defects were filled with the proper volume of graft materials. The periosteum was sutured with 4-0 Vicryl suture threads (Johnson & Johnson Medical GmbH, Norderstedt, Germany). Finally, the skin was sutured with 4-0 Blue Nylon (Ailee Co., Busan, Korea). All rabbits recovered after the operation with no complications and were administered with biotril for 3 days after surgery. Each operation was performed under sterile conditions. At 2, 4, and 8 weeks, rabbits were sacrificed by administering 25 mg/kg of Succipharm (Komipharm Co., Shihung, Korea).

The bone graft granule size, interconnected pores, and granule surface were observed at  $\times 100$  and  $\times 2000$  magnification with SEM (HITACHI S-4300, Hitachi Co., Tokyo, Japan).

The tissues collected from the calvaria were scanned by micro CT (SkyScan 1173, Bruker MicroCT, Kontich, Belgium). The top tissues around the defects were also scanned at a high resolution of  $9.94 \mu\text{m}$ . Pixel images ( $2240 \times 2240$ ) of the scanned tissues were obtained and analyzed. The tissues were wrapped in parafilm before being attached to a zig. All scans were obtained using the following parameters: 130 kV and  $60 \mu\text{A}$ , a brass filter to optimize the contrast,  $180^\circ$  rotation, five frames averaging a rotation step of  $0.2^\circ$ , and ring artifact corrections set at 8. Reconstruction software NRecon ver. 1.6.9.8. (Bruker MicroCT, Konitch, Belgium) was used to create 3D images.

Each tissue specimen was fixed in a formalin solution (neutral buffered, Sigma-Aldrich Co. LLC., St. Louis, MO, USA) for 2 weeks and then dehydrated while increasing the ethanol concentration of the tissue specimen. A mixture of ethanol and Technovit 7200 resin (Heraeus Kulzer, Hanau, Germany) was injected into the dehydrated tissue specimens while the percentage of resin was increased. After penetration was complete, each tissue was separately fixed to an embedment frame and then embedded. For embedment, the specimen was placed in the EXAKT 520 ultraviolet (UV) embedding system (Exakt GmbH, Norderstedt, Germany), and the resin was solidified for 1 day. After the solidification was complete, the desired section of the specimen was attached to a slide with an adhesive press system and the EXAKT 300 CP diamond cutting system (Exakt GmbH, Norderstedt, Germany). The tissue section was then ground to a thickness of  $40 \pm 5 \mu\text{m}$  using the EXAKT 400CS grinding system (Exakt GmbH, Norderstedt, Germany). These tissue specimens were dyed with hematoxylin and eosin and then sealed.

A charge-coupled device (CCD) digital camera system was attached to an optical microscope (BX51, Olympus, Tokyo, Japan) to obtain pictures at a magnification of  $\times 12.5$ , and histomorphometric analysis was conducted at a magnification of  $\times 40$ . To accurately measure the area, magnification was increased to  $\times 100$  as needed. For histomorphometric measurements, multiple images were obtained without overlap from one specimen by saving only the parts shown under the  $\times 40$  optical microscope. The defect area,

the newly formed bone area, and the total bone formation area were measured with Image-Pro plus ver. 4.5 (Media Cybernetics, Inc., Bethesda, MD, USA).

The newly formed bone and total bone formation measurements from the micro CT and histomorphometric analysis were statistically analyzed with SPSS ver. 20.0 (SPSS Inc., Chicago, IL, USA). Median, minimum and maximum values of the bone formation measurements were calculated, and the nonparametric Kruskal-Wallis test was used to compare data from micro CT and histomorphometric analysis. The Dunn procedure was chosen to assess the statistical significance of differences among them. Statistical significance was set at  $P < .05$ .

## RESULTS

All animals recovered after surgery without complications or infections, such as an exposed bone graft, and healed normally during the observation and experimental period.

The shape and surface characteristics of the bone graft materials were observed by SEM at low ( $\times 100$ ) and high ( $\times 2000$ ) magnifications. Fully interconnected pores, approximately  $150 - 200 \mu\text{m}$ , were observed at the lower magnification on the SEM images of Os.  $\beta$ -TCP crystals on the surface were observed at the high magnification.

For Ti, irregularly interconnected pores and micropores were observed within the structure. Interconnected pore sizes were  $150 - 200 \mu\text{m}$ . The granules were generally spherical in shape, and the number of interconnected pores was less than that of Os ( $\times 100$ ). At the high magnification, the granule surfaces were relatively uniform and smooth.

Zi was similar to the above materials in granule size, and the marginal end was very sharp and thin ( $\times 100$ ). The size of the interconnected pores ranged from  $300$  to  $400 \mu\text{m}$ , with their number being fewer and their size being larger than the other graft materials. The surface consisted of uniform granules, which appeared to be polycrystals that formed during the sintering process.

The micro CT analysis results are shown in Table 1, Table 2 and Fig. 1, Fig. 2, Fig. 3. The defect area of the control group could not be measured with micro CT due to the radiolucency of the defect space, so only the newly formed bone volume was measured (in  $\text{mm}^3$ ) to compare with the control group.

The 3D images did not clearly define the formation of

**Table 1.** Micro CT results of area fraction of newly formed bone (unit: %)

Group	Median (min - max)		
	2 weeks	4 weeks	8 weeks
Os	17.78 (14.42 - 22.47)	22.13 (16.52 - 27.18)	21.79 (16.53 - 27.83)
Ti	12.16 (10.30 - 14.31)	21.06 (16.22 - 25.13)	23.10 (18.05 - 27.44)
Zi	12.29 (9.96 - 15.06)	18.28 (15.65 - 22.64)	18.76 (17.78 - 25.79)

**Table 2.** Micro CT results of the area fraction of total bone (unit: %)

Group	Median (min - max)		
	2 weeks	4 weeks	8 weeks
Os	44.22 (36.13 - 52.43)	53.95 (44.12 - 62.01)	44.71 (42.63 - 57.49)
Ti	79.50 (57.24 - 85.02)	73.51 (57.21 - 80.67)	88.72 (64.28 - 92.10)
Zi	73.82 (68.28 - 83.54)	87.61 (66.25 - 92.15)	85.34 (71.18 - 91.01)

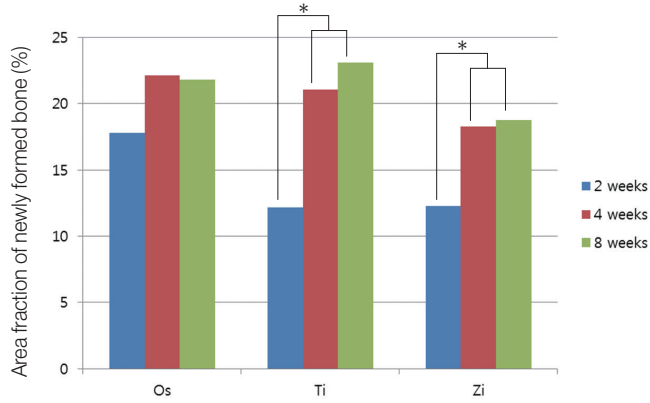


**Fig. 1.** Micro CT results of area fraction of newly formed bone. \* denotes significant difference at 0.05.

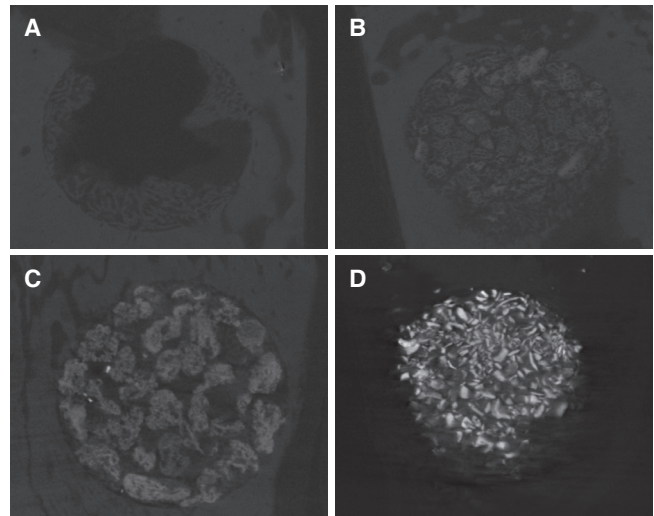


**Fig. 2.** Micro CT results of the cranial defects in rabbits 2 weeks postsurgery. (A) Control, (B) Osteon II, (C) Tigran PTG, (D) Zirconia graft material.

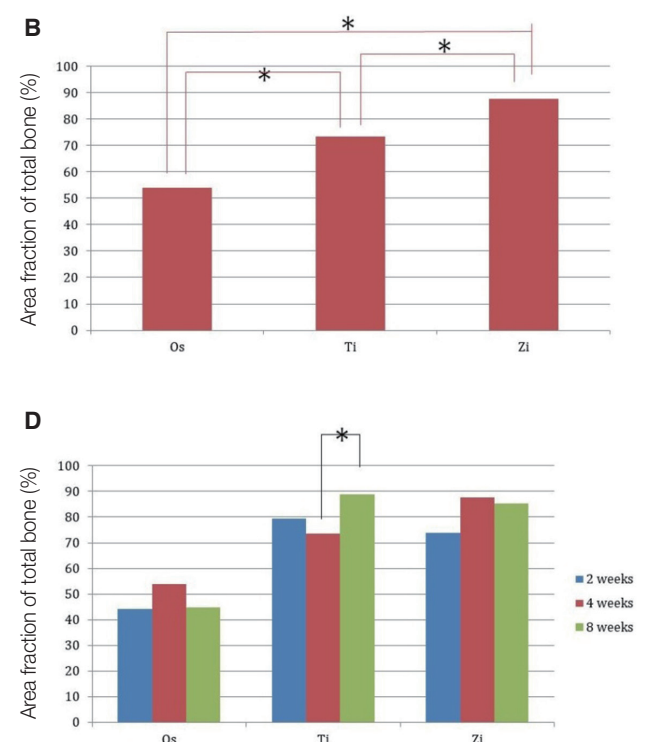
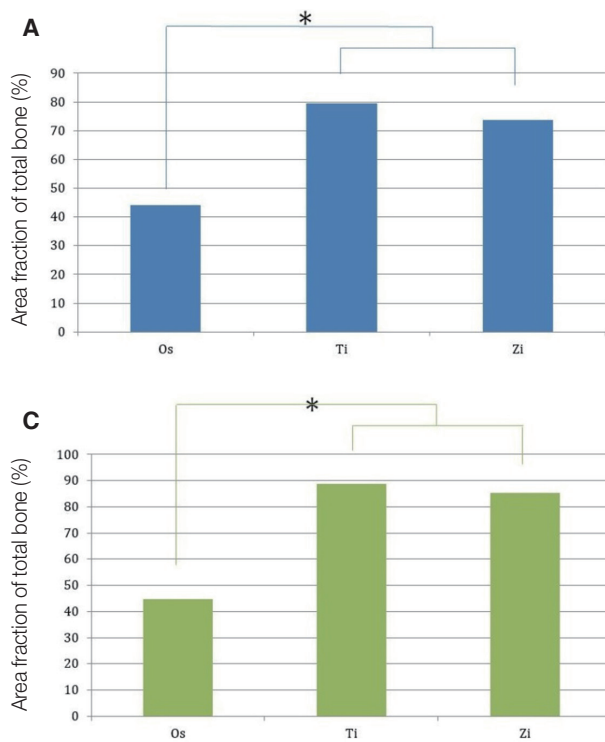


**Fig. 3.** (A) Micro CT results of area fraction of total bone at 2 weeks, (B) Micro CT results of area fraction of total bone at 4 weeks, (C) Micro CT results of area fraction of total bone at 8 weeks, (D) Micro CT results of area fraction of total bone. \* denotes significant difference at 0.05.

new bone in the grafted bone, but the control group showed new bones being formed from the margin of the defects. The amount of newly formed bone gradually increased over time, and well-organized lamellar bone islands appeared at the center of the defect at 8 weeks.

Newly formed bone was calculated as the percentage of the total defects in order to compare bone formation among experimental groups and weeks shown in Table 1.

At 2 weeks, the amount of total bone of the Os group was much less than that of the Ti and Zi groups, and the difference was significant ( $P < .05$ ). At 4 weeks, all groups showed significant differences in total bone formation ( $P < .05$ ). At 8 weeks, the Os group showed significant differences with the Ti and Zi groups. The amount of total bone of the Os group was the least among the experimental groups.

Total bone was calculated as the percentage of the defects in order to compare total bone formation among experimental groups and weeks shown in Table 2.

As shown in Fig. 2, there was different tendency of bone formation between groups at 2 weeks.

As shown in Fig. 3D, there was a significant difference between week 4 and week 8 for the Ti group ( $P < .05$ ), but no significant differences were found in the other groups.

The histomorphometric results are shown in Table 3, Table 4 and Fig. 4, Fig. 5, Fig. 6, Fig. 7, Fig. 8. At 2 weeks, newly formed bone was observed in the peripheral portion of the defects in all groups (Fig. 4). At 4 weeks, the space

between the granules was more occupied by newly formed bone than 2 weeks in the experimental groups (Fig. 5). At 8 weeks, a lamellar bone island was seen in the control group, and the amount of newly formed bone gradually increased from the margin to the center of the defects in all experimental groups (Fig. 6).

Newly formed bone and total bone formation was converted to percentages, as described previously, and compared among groups and weeks.

A comparison of the amount of newly formed bone at each week is shown in Fig. 7A to Fig. 7C. There were significant differences between the control group and experimental groups for all weeks ( $P < .05$ ). A comparison between experimental groups showed no significant difference. A comparison of the amount of newly formed bone by week in each group is shown in Fig. 7D. For all groups, significant differences only existed between 2 and 4 weeks and between 2 and 8 weeks ( $P < .05$ ). Among these groups, the Ti group showed a decrease in newly formed bone at week 8 compared to week 4.

A comparison of total bone among groups is shown in Fig. 8A to Fig. 8C. Inter-group comparisons confirmed significant differences among groups at every week ( $P < .05$ ).

In the comparison among weeks, the control group showed significant differences between 2 and 4 weeks, and between 2 and 8 weeks ( $P < .05$ ). There was no statistical significance by week for the experimental groups.

**Table 3.** Histomorphometric results of the area fraction of newly formed bone (unit: %)

Group	Median (min - max)		
	2 weeks	4 weeks	8 weeks
Control	5.03 (3.98 - 5.85)	7.68 (5.97 - 8.74)	9.68 (7.75 - 11.39)
Os	11.96 (10.21 - 13.98)	16.01 (12.97 - 17.81)	17.86 (13.98 - 21.30)
Ti	11.73 (9.48 - 14.62)	17.01 (12.19 - 21.64)	15.97 (12.67 - 20.07)
Zi	13.62 (10.87 - 15.86)	17.30 (12.47 - 19.60)	17.70 (14.35 - 21.15)

**Table 4.** Histomorphometric results of the area fraction of total bone (unit: %)

Group	Median (min - max)		
	2 weeks	4 weeks	8 weeks
Control	5.03 (3.98 - 5.85)	7.68 (5.97 - 8.74)	9.68 (7.75 - 11.39)
Os	39.97 (32.38 - 46.72)	43.40 (32.50 - 49.26)	47.67 (37.82 - 50.48)
Ti	51.21 (42.81 - 58.21)	58.86 (46.06 - 60.81)	57.57 (47.59 - 63.87)
Zi	64.91 (54.41 - 68.61)	69.50 (57.49 - 75.40)	69.57 (58.32 - 76.02)

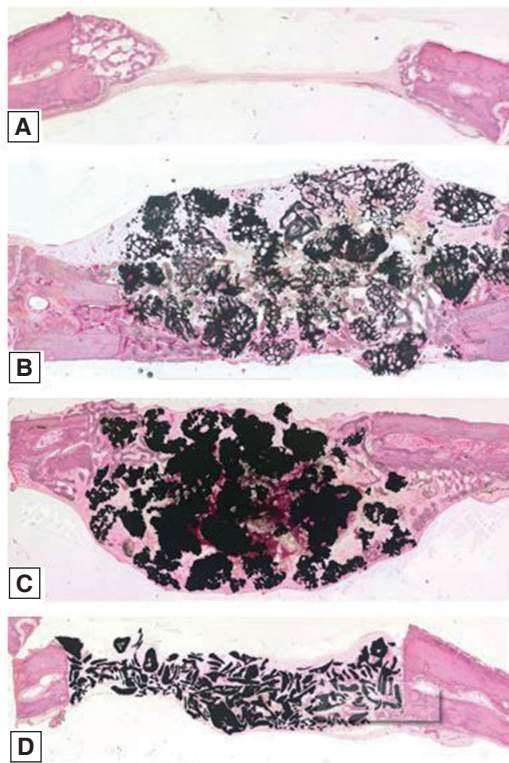


**Fig. 4.** Histological sections of the cranial defects in rabbits 2 weeks postsurgery. (A) Control, (B) Osteon II, (C) Tigran PTG, (D) Zirconia graft material.

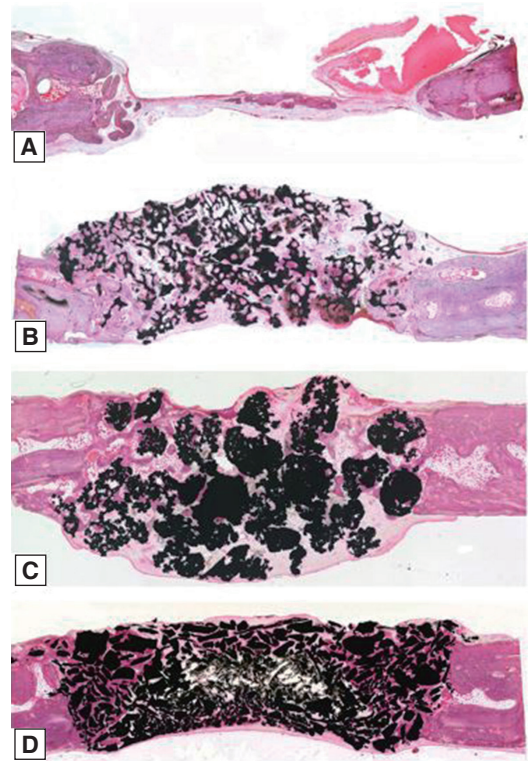


**Fig. 6.** Histological sections of the cranial defects in rabbits 8 weeks postsurgery. (A) Control, (B) Osteon II, (C) Tigran PTG, (D) Zirconia graft material.

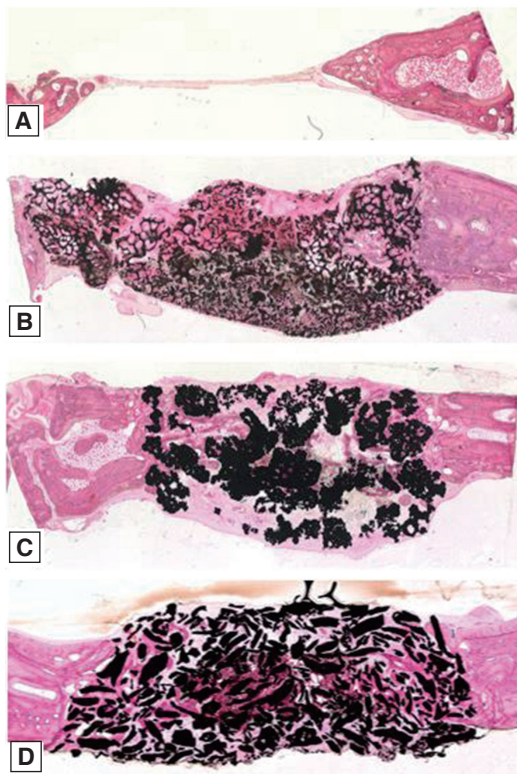


**Fig. 5.** Histological sections of the cranial defects in rabbits 4 weeks postsurgery. (A) Control, (B) Osteon II, (C) Tigran PTG, (D) Zirconia graft material.

## DISCUSSION

Zirconia was shown to help the proliferation of osteoblasts, and results from other experimental studies<sup>28-31</sup> have confirmed that the zirconia implant has good biocompatibility. Y-TZP graft material in this study was produced using powdered slurry water as recommended by Song and Cho.<sup>28</sup> Y-TZP is an advantageous material that maintains bone graft volume, in contrast with other materials,<sup>7,17</sup> and minimizes fractures from unnecessary pressure during the healing period due to its compressive strength.<sup>32</sup> With these properties and the need to obtain predictable results, Y-TZP would be the better choice as a bone graft material in the oral and maxillofacial region.

Rabbit experiments can provide a faster and reliable result than other animal studies due to faster bone-healing process<sup>33</sup> and similar genetic traits. Calvaria of rabbit were selected to obtain uniform results while preventing unnecessary pressure to the bone grafted site. The defect size was designed to a diameter of 6 mm for the rabbit's safety, shorter healing time,<sup>34</sup> and elimination of unnecessary pressure. The specimens were collected to examine bone healing and remodeling at 2 weeks. Likewise, the specimens were collected at 4 weeks to show new bone ingrowth and at 8 weeks to observe the maturation of new bone.

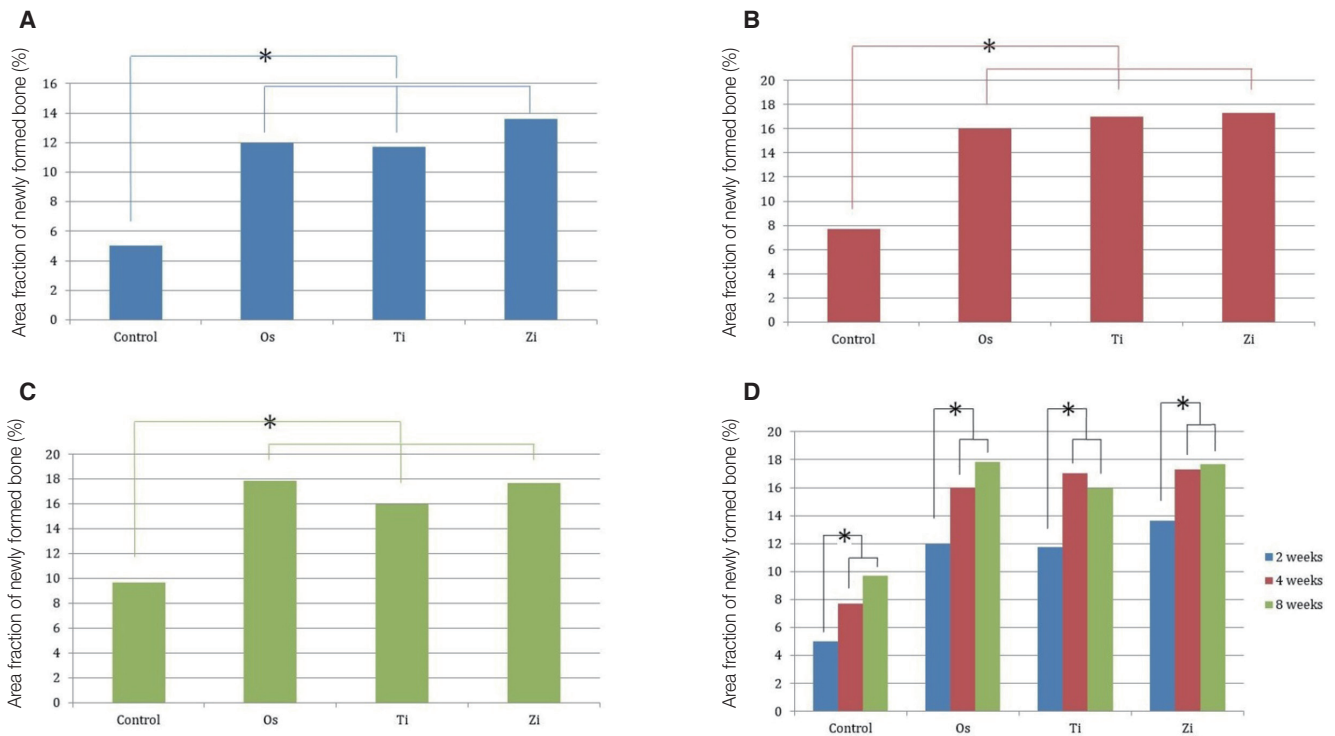


**Fig. 7.** (A) Histomorphometric results of the area fraction of newly formed bone at 2 weeks, (B) Histomorphometric results of the area fraction of newly formed bone at 4 weeks, (C) Histomorphometric results of the area fraction of newly formed bone at 8 weeks, (D) Histomorphometric results of the area fraction of newly formed bone. \* denotes significant difference at 0.05.

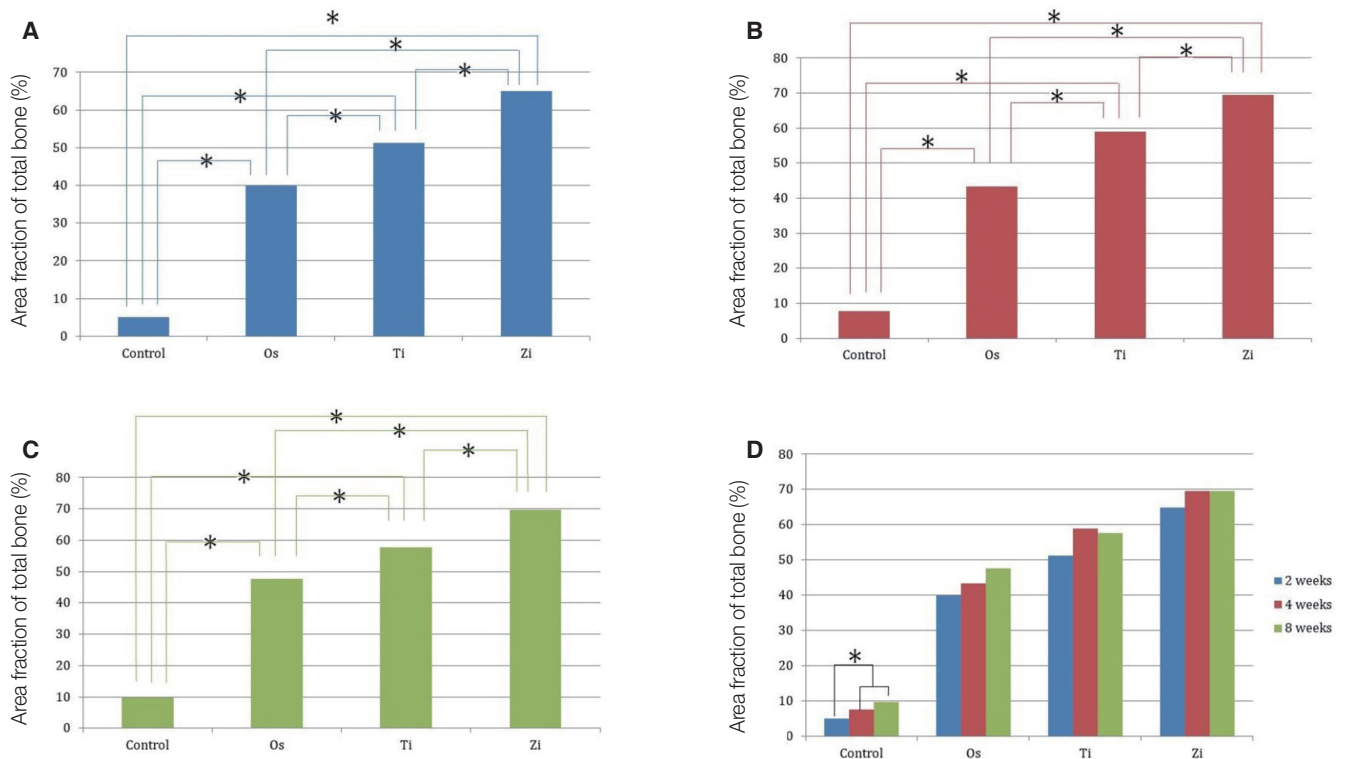


**Fig. 8.** (A) Histomorphometric results of the area fraction of total bone at 2 weeks, (B) Histomorphometric results of the area fraction of total bone at 4 weeks, (C) Histomorphometric results of the area fraction of total bone at 8 weeks, (D) Histomorphometric results of the area fraction of total bone. \* denotes significant difference at 0.05.

The bone graft materials of the experimental groups used in this study were produced with different materials by different manufacturers. To derive consistent experimental results, granules and interconnected pores of the bone graft materials were designed to have a similar size. A granule size of 0.5 to 1.0 mm, which is mainly used for oral and maxillofacial surgeries, and an interconnected pore size of 150 to 500  $\mu\text{m}$ , which is the proper size for new bone formation, were chosen.<sup>20-22</sup> In the case of Zi, similar sizes of bone graft materials could be obtained by using experimental sieves.<sup>28</sup> However, the interconnected pore size of Zi was uneven and larger than that of the other experimental groups. The granule sizes and interconnected pores were checked by the manufacturers' guidelines and by SEM measurements. In the current study, a membrane coverage was not required because the graft materials maintained their original position and volume,<sup>35,36</sup> and using a membrane increases the risk of infection and can lead to a foreign body reaction.<sup>37,38</sup>

Os was chosen as a synthetic bone graft material in this study because it has a similar shape and composition to human bones.<sup>39,40</sup> Also, titanium bone graft material was chosen due to unique biocompatibility, biological inactivity, a non-absorbable property, and mechanical strength.<sup>41-45</sup> However, SEM observations showed that Ti granule has low pore connectivity. Histologically, the relatively small micropores and space inside the granules were not considered sufficient to promote new bone formation.

Based on the SEM photographs, the bone graft materials of all experimental groups showed similar granule sizes in general. However, the margins of Zi were sharp and thin and the sizes of the interconnected pores were not uniform. The initial form of zirconia was a cribriform block with the same shape as polyurethane. The sharp edges were generated in the production process and formed while the blocks were being crushed to produce granules. Moreover, it was difficult to obtain uniform interconnected pores during crushing process. Sharp edges were presumed to cause unnecessary irritation to soft tissues and might delay healing of the soft tissues and cause problems in new bone formation in animal experiments. However, no inflammation occurred during the experimental periods, suggesting that the sharp edges did not interfere with new bone formation. Based on the results, better bone formation would be expected if the production method could be improved to eliminate the stimulation of tissues by sharp edges.

It was difficult to measure the exact amounts of newly formed bone using micro CT because each bone graft material had different radiopacity, artifact images limited the verification of the new bone, and micro CT was susceptible to various conditions.<sup>46,47</sup> Nevertheless, the tendency of bone formation was found. Therefore, comparisons of the newly formed bone and total bone volume with micro CT were appropriate among weeks within a group and these were considered meaningful results. Histomorphometric analysis provided more objective and consistent results compared to micro CT analysis.

Histomorphometric analysis after 2 weeks showed new

bone formation in most cases. The experimental groups showed a large amount of newly formed bones compared to the control group, but the results were not significant among the experimental groups. The patterns of early bone formation in this study are in agreement with those of a previous study of bone grafts to bone defects on rabbit calvaria.

Histomorphometric analysis of the total bone formation area showed that significant differences among all groups existed for every period ( $P < .05$ ). This difference was due to new bone formation as well as the different porosity of the bone graft materials. The Zi bone graft images showed an insufficient distance for new bone ingrowth between the granules compare to those of other bone graft materials, and this seems to be associated with the shape of the Zi granules. Unlike other granules that have a spherical shape, the Zi graft material was atypical, with an irregular form and had sharp edges that could densely fill the spaces between granules. If zirconia bone graft material could be produced as spherical granules with similar shapes, better comparisons could be made with other experimental groups. Recent studies have documented the formation of new bones through zirconia surface treatment, and bone grafting with zirconia could be developed more effectively.<sup>48-50</sup>

Biocompatibility, non-absorbability, and esthetics of zirconia are well suited for the current trends in dental clinical practice. In particular, it is expected that zirconia will show good results during maxillofacial rehabilitation and dental implant surgery that require bone grafting using 3D images. Further studies will be required to confirm the use of zirconia as a new bone graft material by comparing it with conventional bone graft materials.

## CONCLUSION

Based on the above findings, the zirconia bone graft material showed satisfactory results in new bone formation compared to other bone graft materials and therefore could be used as a new synthetic bone graft material in clinical practice.

## ORCID

Ik-Jung Kim <https://orcid.org/0000-0003-1246-5019>

Soo-Yeon Shin <https://orcid.org/0000-0001-6160-7277>

## REFERENCES

1. Marx RE. Clinical application of bone biology to mandibular and maxillary reconstruction. *Clin Plast Surg* 1994;21:377-92.
2. Hoexter DL. Bone regeneration graft materials. *J Oral Implantol* 2002;28:290-4.
3. Quattlebaum JB, Mellonig JT, Hensel NF. Antigenicity of freeze-dried cortical bone allograft in human periodontal osseous defects. *J Periodontol* 1988;59:394-7.
4. Sogal A, Tofe AJ. Risk assessment of bovine spongiform encephalopathy transmission through bone graft material derived from bovine bone used for dental applications. *J Periodontol* 1999;70:1053-63.



5. Vaccaro AR. The role of the osteoconductive scaffold in synthetic bone graft. *Orthopedics* 2002;25:s571-8.
6. Tadic D, Epple M. A thorough physicochemical characterisation of 14 calcium phosphate-based bone substitution materials in comparison to natural bone. *Biomaterials* 2004;25:987-94.
7. Kondo N, Ogose A, Tokunaga K, Ito T, Arai K, Kudo N, Inoue H, Irie H, Endo N. Bone formation and resorption of highly purified beta-tricalcium phosphate in the rat femoral condyle. *Biomaterials* 2005;26:5600-8.
8. Gholami GA, Tehranchi M, Kadkhodazadeh M, Moghadam AA, Ghanavati F, Ardakani MRT, Aghaloo M, Mashhadiabbas F. Histologic and histomorphometric evaluation of bone substitutes in experimental defects. *Res J Biol Sci* 2010;5:465-9.
9. Bystedt H, Rasmusson L. Porous titanium granules used as osteoconductive material for sinus floor augmentation: a clinical pilot study. *Clin Implant Dent Relat Res* 2009;11:101-5.
10. Al-Sabbagh M. Implants in the esthetic zone. *Dent Clin North Am* 2006;50:391-407.
11. Wenz HJ, Bartsch J, Wolfart S, Kern M. Osseointegration and clinical success of zirconia dental implants: a systematic review. *Int J Prosthodont* 2008;21:27-36.
12. Sollazzo V, Pezzetti F, Scarano A, Piattelli A, Bignozzi CA, Massari L, Brunelli G, Carinci F. Zirconium oxide coating improves implant osseointegration in vivo. *Dent Mater* 2008;24:357-61.
13. Brüll F, van Winkelhoff AJ, Cune MS. Zirconia dental implants: a clinical, radiographic, and microbiologic evaluation up to 3 years. *Int J Oral Maxillofac Implants* 2014;29:914-20.
14. Sennerby L, Dasmah A, Larsson B, Iverhed M. Bone tissue responses to surface-modified zirconia implants: A histomorphometric and removal torque study in the rabbit. *Clin Implant Dent Relat Res* 2005;7:S13-20.
15. Piconi C, Maccauro G. Zirconia as a ceramic biomaterial. *Biomaterials* 1999;20:1-25.
16. Gredes T, Kubasiewicz-Ross P, Gedrange T, Dominiak M, Kunert-Keil C. Comparison of surface modified zirconia implants with commercially available zirconium and titanium implants: a histological study in pigs. *Implant Dent* 2014;23:502-7.
17. Depprich R, Zipprich H, Ommerborn M, Mahn E, Lammers L, Handschel J, Naujoks C, Wiesmann HP, Kübler NR, Meyer U. Osseointegration of zirconia implants: an SEM observation of the bone-implant interface. *Head Face Med* 2008;4:25.
18. Garvie RC, Hannink RH, Pascoe RT. Ceramic steel? *Nature* 1975;258:703-4.
19. Pae AR, Lee HS, Kim HS, Baik J, Woo YH. Cellular attachment and gene expression of osteoblast-like cells on zirconia ceramic surfaces. *J Korean Acad Prosthodont* 2008;43:227-37.
20. Guazzato M, Quach L, Albakry M, Swain MV. Influence of surface and heat treatments on the flexural strength of Y-TZP dental ceramic. *J Dent* 2005;33:9-18.
21. Kim YK, Kim SG, Kim BS, Jeong KI. Resorption of bone graft after maxillary sinus grafting and simultaneous implant placement. *J Korean Assoc Oral Maxillofac Surg* 2014;40:117-22.
22. Silva NR, Sailer I, Zhang Y, Coelho PG, Guess PC, Zembic A, Kohal RJ. Performance of zirconia for dental healthcare. *Materials* 2010;3:863-96.
23. Orentlicher G, Goldsmith D, Abboud M. Computer-guided planning and placement of dental implants. *Atlas Oral Maxillofac Surg Clin North Am* 2012;20:53-79.
24. Gahleitner A, Watzek G, Imhof H. Dental CT: imaging technique, anatomy, and pathologic conditions of the jaws. *Eur Radiol* 2003;13:366-76.
25. Xu H, Shimizu Y, Asai S, Ooya K. Experimental sinus grafting with the use of deproteinized bone particles of different sizes. *Clin Oral Implants Res* 2003;14:548-55.
26. Klawitter JJ, Hulbert SF. Application of porous ceramics for the attachment of load bearing internal orthopedic applications. *J Biomed Mater Res* 1971;5:161-229.
27. Huh JB, Jung DH, Kim JS, Shin SW. Effects of different sizes of Hydroxyapatite/ $\beta$ -Tricalcium phosphate particles on vertical bone augmentation. *J Korean Acad Prosthodont* 2010;48:259-65.
28. Song YG, Cho IH. Characteristics and osteogenic effect of zirconia porous scaffold coated with  $\beta$ -TCP/HA. *J Adv Prosthodont* 2014;6:285-94.
29. Langhoff JD, Voelter K, Scharnweber D, Schnabelrauch M, Schlottig F, Hefti T, Kalchofner K, Nuss K, von Rechenberg B. Comparison of chemically and pharmaceutically modified titanium and zirconia implant surfaces in dentistry: a study in sheep. *Int J Oral Maxillofac Surg* 2008;37:1125-32.
30. Scarano A, Di Carlo F, Quaranta M, Piattelli A. Bone response to zirconia ceramic implants: an experimental study in rabbits. *J Oral Implantol* 2003;29:8-12.
31. Kohal RJ, Weng D, Bächle M, Strub JR. Loaded custom-made zirconia and titanium implants show similar osseointegration: an animal experiment. *J Periodontol* 2004;75:1262-8.
32. Pilathadka S, Vahalová D, Vosáhlo T. The Zirconia: a new dental ceramic material. An overview. *Prague Med Rep* 2007;108:5-12.
33. Roberts EW, Poon LC, Smith RK. Interface histology of rigid endosseous implants. *J Oral Implantol* 1986;12:406-16.
34. Sohn JY, Park JC, Um YJ, Jung UW, Kim CS, Cho KS, Choi SH. Spontaneous healing capacity of rabbit cranial defects of various sizes. *J Periodontal Implant Sci* 2010;40:180-7.
35. Becker W, Becker BE, Handelsman M, Ochsenschein C, Albrektsson T. Guided tissue regeneration for implants placed into extraction sockets: a study in dogs. *J Periodontol* 1991;62:703-9.
36. Buser D, Hoffmann B, Bernard JP, Lussi A, Mettler D, Schenk RK. Evaluation of filling materials in membrane-protected bone defects. A comparative histomorphometric study in the mandible of miniature pigs. *Clin Oral Implants Res* 1998;9:137-50.
37. Gotfredsen K, Nimb L, Hjørtting-Hansen E. Immediate implant placement using a biodegradable barrier, polyhydroxybutyrate-hydroxyvalerate reinforced with polyglactin 910. An experimental study in dogs. *Clin Oral Implants Res* 1994;5:83-91.
38. Hämmerle CH, Jung RE. Bone augmentation by means of

- barrier membranes. *Periodontol* 2000 2003;33:36-53.
39. LeGeros RZ, Lin S, Rohanizadeh R, Mijares D, LeGeros JP. Biphasic calcium phosphate bioceramics: preparation, properties and applications. *J Mater Sci Mater Med* 2003;14:201-9.
  40. Kim YK, Yun PY, Lim SC, Kim SG, Lee HJ, Ong JL. Clinical evaluations of OSTEON as a new alloplastic material in sinus bone grafting and its effect on bone healing. *J Biomed Mater Res B Appl Biomater* 2008;86:270-7.
  41. Branemark PI, Zarb GA, Albrektsson T. Tissue integrated prostheses: Osseointegration in clinical dentistry. 1<sup>st</sup> ed. Quintessence Pub Co.; 1985. p. 221-9.
  42. Albrektsson T, Brånemark PI, Hansson HA, Lindström J. Osseointegrated titanium implants. Requirements for ensuring a long-lasting, direct bone-to-implant anchorage in man. *Acta Orthop Scand* 1981;52:155-70.
  43. Brånemark PI, Hansson BO, Adell R, Breine U, Lindström J, Hallén O, Ohman A. Osseointegrated implants in the treatment of the edentulous jaw. Experience from a 10-year period. *Scand J Plast Reconstr Surg Suppl* 1977;16:1-132.
  44. Wohlfahrt JC, Monjo M, Rønold HJ, Aass AM, Ellingsen JE, Lyngstadaas SP. Porous titanium granules promote bone healing and growth in rabbit tibia peri-implant osseous defects. *Clin Oral Implants Res* 2010;21:165-73.
  45. Thor A. Porous titanium granules and blood for bone regeneration around dental implants: Report of four cases and review of the literature. *Case Rep Dent* 2013;2013:410515.
  46. Meganck JA, Kozloff KM, Thornton MM, Broski SM, Goldstein SA. Beam hardening artifacts in micro-computed tomography scanning can be reduced by X-ray beam filtration and the resulting images can be used to accurately measure BMD. *Bone* 2009;45:1104-16.
  47. Ejima K, Omasa S, Motoyoshi M, Arai Y, Kai Y, Amemiya T, Yamada H, Honda K, Shimizu N. Influence of metal artifacts on in vivo micro-CT for orthodontic mini-implants. *J Oral Sci* 2012;54:55-9.
  48. Kim HW, Georgiou G, Knowles JC, Koh YH, Kim HE. Calcium phosphates and glass composite coatings on zirconia for enhanced biocompatibility. *Biomaterials* 2004;25:4203-13.
  49. Kim HW, Lee SY, Bae CJ, Noh YJ, Kim HE, Kim HM, Ko JS. Porous ZrO<sub>2</sub> bone scaffold coated with hydroxyapatite with fluorapatite intermediate layer. *Biomaterials* 2003;24:3277-84.
  50. Kim HW, Kim HE, Salih V, Knowles JC. Dissolution control and cellular responses of calcium phosphate coatings on zirconia porous scaffold. *J Biomed Mater Res A* 2004;68:522-30.